Zero-temperature statics and dynamics of a random-exchange model for magnetic properties of $La_{2-x}Sr_xCuO_4$ in the insulating regime

W. Y. Ching
Department of Physics, University of Missouri–Kansas City, Kansas City, Missouri 64110

D. L. Huber
Department of Physics, University of Wisconsin–Madison, Madison, Wisconsin 53706
(Received 26 January 1990)

Results are presented for the zero-temperature statics and dynamics of a random-exchange model proposed for the magnetic properties of $La_{2-x}Sr_xCuO_4$. Numerical calculations of the staggered magnetization, the static structure factor, the distribution and localization of the harmonic magnon modes, and the dynamic structure factor are reported for $c \ll 1$, where c is the fraction of ferromagnetic exchange integrals in an otherwise perfect two-dimensional antiferromagnetic array with nearest-neighbor Heisenberg interactions. The relevance of the findings to the magnetic behavior of $La_{2-x}Sr_xCuO_4$ in the insulating regime is assessed. It is pointed out that the model accounts for the crossover from antiferromagnetic to spin-glass behavior, the broadening of the static structure factor, and the renormalization of the spin-wave modes that occur with increasing hole concentration at low temperatures.

I. INTRODUCTION

The discovery and subsequent study of high-T_c materials has stimulated the development of numerous microscopic models for their properties. In such a situation, it is important to test the predictions of the models against experiment, since the results of these tests may make it possible to eliminate candidate theories.

In this paper, we will focus on the low-temperature magnetic properties of $La_{2-x}Sr_xCuO_4$ in the insulating regime and, specifically, on a model introduced by Aharony *et al.* to explain the magnetic phase diagram.[1,2] The essential feature of the model is the assumption that the introduction of a small number of holes in the Cu-O planes, brought about by doping with Sr, produces a short-range ferromagnetic exchange interaction between the Cu^{2+} spins that tends to destroy the antiferromagnetic order characteristic of the undoped material. At low temperatures, as the hole concentration increases, the system passes from an antiferromagnetic to a spin-glass-like state and, ultimately, undergoes a metal-insulator transition into the superconducting phase at a strontium concentration corresponding to $x \approx 0.06$.

The magnetic properties of undoped La_2CuO_4 are well characterized by the Heisenberg Hamiltonian

$$\mathcal{H} = \sum_{(i,j)} J_{ij}\mathbf{S}_i \cdot \mathbf{S}_j \ , \tag{1}$$

where $\mathbf{S}_i$ is the spin of the Cu^{2+} ion ($S = \frac{1}{2}$) and J_{ij} is the exchange interaction between spins on sites i and j. The dominant interaction is an antiferromagnetic coupling between nearest neighbors in the Cu-O planes for which $J_{ij} = 0.12$–0.16 eV.[3,4]

In the insulating regime, the holes are immobile at very low temperatures. Aharony *et al.*[1] assume they reside on the O sites that are midway between the Cu ions. The location of the holes is consistent with the theory of Emery[5] but differs from the underlying picture of the t-J model where the holes form singlet states with the Cu ions.[6] A hole on the oxygen will interact with the Cu ions and, thus, affect the exchange interactions. The critical feature of the model introduced in Ref. 1 is the assumption that a hole on an oxygen site between two Cu spins introduces a strong *ferromagnetic* exchange interaction between them.

The Hamiltonian associated with this model takes the form

$$\mathcal{H} = \sum_{(i,j)}{}' J_{ij}\mathbf{S}_i \cdot \mathbf{S}_j \ , \tag{2}$$

where the prime signifies that the sum is limited to nearest neighbors on a square lattice. In Eq. (2), $J_{ij} = J\,(J > 0)$ if there is no hole on the oxygen site between the Cu ions and $J_{ij} = -K\,(K > 0)$, if there is a hole on the oxygen site. In Ref. 1, arguments are given for $K/J \gg 1$. The question we are addressing is whether this Hamiltonian can account for the magnetic properties of $La_{2-x}Sr_xCuO_4$ in the insulating regime. More specifically, is the model an adequate first approximation for describing the effect of the holes on the statics and dynamics of the Cu spins at low temperatures?

This paper reports the results of an investigation of the zero-temperature behavior associated with the Hamiltonian displayed in Eq. (2) with a small concentration, c, of random distributed ferromagnetic interactions. (We reserve the variable x for the Sr concentration.) A preliminary report on the effects of the ferromagnetic interactions on the staggered magnetization and static structure factor was given in Ref. 7. After reviewing that work, we will concentrate on the dynamical aspects of

the model. The results of numerical calculations of the distribution and localization of the magnon modes and the zero-temperature dynamic structure factor are presented for $c=0.01$, 0.05, and 0.10.

Our approach to the problem is based on large scale calculations of the properties of finite arrays of spins. Apart from those inherent in the starting Hamiltonian, our principal approximation is to neglect quantum fluctuations and work within the framework of a classical (Nèel-like) ground state and harmonic (linear) spin-wave theory. Although both of these are severe approximations for two-dimensional, spin-$\frac{1}{2}$ systems, nevertheless, there is experimental and theoretical evidence that they provide a reasonable starting point for a "first-approximation" characterization of the statics and dynamics in undoped La_2CuO_4.[4,8,9]

Recent studies have shown that our methods can account for the neutron scattering from three-dimensional dilute magnetic semiconductors in the spin-glass regime,[10] and the quasi-two-dimensional magnet $Rb_2Mn_xCr_{1-x}Cl_4$,[11] which, like the model under study, has competing ferromagnetic and antiferromagnetic interactions. Apart from the question of quantum corrections, we expect a similar degree of success from our analysis of the random bond model. Judging from the situation in La_2CuO_4, we anticipate that a fully quantum-mechanical calculation would produce results which were *qualitatively* similar, but differed quantitatively on the order of 20%, a scale set by the effect of quantum fluctuations on the zero-temperature staggered magnetization and spin-wave velocity of the two-dimensional Heisenberg antiferromagnet.

The remainder of this paper is divided into four sections. Section II is a summary of the pertinent results for the static properties presented in Ref. 7. The distribution and localization of the magnon modes are given in Sec. III, while the calculation of the dynamic structure factor is outlined in Sec. IV. Section V is devoted to a discussion of our findings and their relation to experimental studies.

II. STATIC BEHAVIOR

The starting point in the analysis is the establishment of equilibrium spin configurations of the corresponding classical spins for various distributions of ferromagnetic bonds. In this step, we followed the approach of Walker and Walstedt[12] in consecutively rotating the spins into the directions of their local fields until the total energy stabilizes to 1 part in 10^8. With the configurations in hand, it is possible to calculate a variety of equilibrium properties. Of particular importance are the staggered magnetization and the static structure factor.

We have carried out a series of calculations of both the staggered magnetization and the structure factor for $K/J=3$. Representative calculations of the staggered magnetization were also carried out for other values of the ratio, and it was found that quantitatively similar behavior was obtained as long as $K/J>1$.[7]

The staggered magnetization associated with a particular equilibrium spin configuration is obtained from the expression

$$M_S=N^{-1}\left[\sum_{\alpha=x,y,z}\left[\sum_i^A n_i^\alpha-\sum_j^B n_j^\alpha\right]^2\right]^{1/2}, \tag{3}$$

where $\hat{\mathbf{n}}_i$ ($\hat{\mathbf{n}}_j$) is a unit vector pointing in the equilibrium direction of the ith (jth) spin on the A (B) sublattice and N is the number of spins. The average and standard deviation of the staggered magnetization obtained from 10 configurations of 80×80 spins are displayed in Table I. From the table it is evident that the introduction of 1% ferromagnetic interactions produces an approximately 28% reduction in the staggered moment ($M_S=1$ for $c=0$). Such a result is consistent with the analysis of Parker and Saslow[13] and Vannimenus *et al.*[14] The latter authors used an effective-medium approach to establish a critical concentration, $c_{cr}(K/J)$, at which widespread noncolinearity of the spins first appears. According to their analysis, in two dimensions, $c_{cr}=0$ for $K/J\geq1$, which suggests that even a very low concentration of "wrong sign" interactions will reduce the staggered magnetization by a significant amount when the strength of the ferromagnetic coupling exceeds the antiferromagnetic interaction. We note that the rapid decrease in the staggered magnetization with increasing c is qualitatively consistent with the crossover from antiferromagnetic to spin-glass-like behavior in $La_{2-x}Sr_xCuO_4$ that was discussed in Ref. 1.

The static structure factor, $S(\mathbf{q})$, is obtained from the Fourier transforms of the unit vectors associated with the equilibrium spin configurations according to the equations

$$\mathbf{n}(\mathbf{q})=\sum_j e^{i\mathbf{q}\cdot\mathbf{r}_j}\hat{\mathbf{n}}_j\ , \tag{4}$$

$$S(\mathbf{q})=N^{-1}\mathbf{n}(\mathbf{q})\cdot\mathbf{n}(-\mathbf{q})\ . \tag{5}$$

In our studies we focused on the neighborhood of the superlattice point $\pi(1,1)$ associated with antiferromagnetic long-range order. The calculations were carried out for $\mathbf{q}$ along [1,1] according to the prescription $\mathbf{q}=\pi(1+Q,1+Q)$, $0\leq Q\leq1$.

The results for $c=0.05$, 0.10, and 0.15 are shown in Fig. 1. The data are obtained by averaging over 30 configurations of 60×60 arrays and 10 configurations of

TABLE I. Calculated values of the staggered magnetization as a function of the fraction, c, of ferromagnetic exchange interactions for 80×80 arrays with $K/J=3$.

c	M_S[a]	ΔM_S[a]
0.01	0.725	0.221
0.05	0.193	0.062
0.10	0.071	0.029
0.15	0.035	0.022
0.20	0.026	0.010
0.25	0.019	0.008

[a] Average (M_S) and standard deviation (ΔM_S) of the staggered magnetization obtained from 10 configurations of randomly distributed ferromagnetic interactions.

80×80 arrays. In all cases $K/J=3$. The data show very clearly that a small concentration of ferromagnetic interactions has a substantial effect on the Bragg peak. In addition to the overall broadening of the peak, a shoulder develops in the neighborhood of $Q=0.1$. Although varying less rapidly with impurity concentration, the behavior of the structure factor is qualitatively similar to neutron-scattering data for $La_{2-x}Sr_xCuO_4$ reported by Birgeneau *et al.*[15]

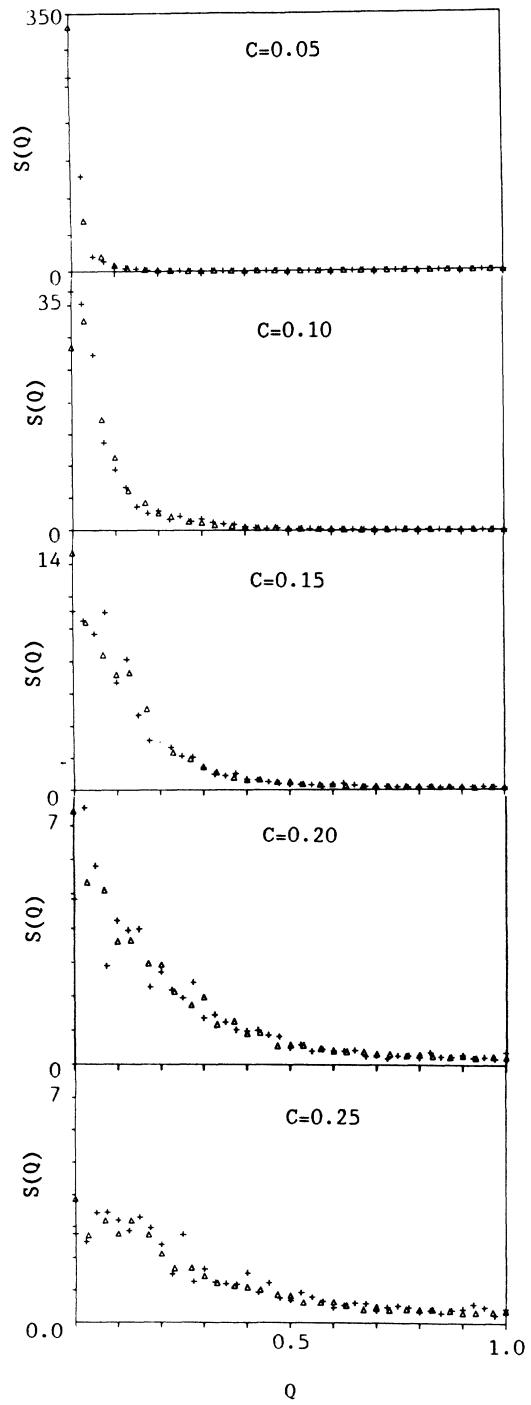

FIG. 1. Static structure factor vs Q. Q is related to the wave vector by $\mathbf{q}=\pi(1+Q,1+Q)$. + average of 10 configurations in 80×80 arrays, △ average of 30 configurations in 60×60 arrays. $c=0.05$, 0.10, 0.15, 0.20, and 0.25. Note change in vertical scale.

One can infer an effective inverse spin-correlation length, κ, from the half-width at half maximum of the peak in $S(Q)$ according to the equation $\kappa=\sqrt{2}\pi$ times the HWHM (Lorentzian approximation). From Fig. 1 we obtain the values $c=0.05$, $\kappa=0.11$; $c=0.10$, $\kappa=0.31$; $c=0.15$, $\kappa=0.66$; $c=0.20$, $\kappa=0.88$; $c=0.25$, $\kappa=1.1$, where κ is in units of the reciprocal of the lattice constant of the spin array. The rapid increase in κ is consistent with the falloff in the staggered magnetization displayed in Table I, while the magnitude indicates that the correlation length is on the order of the average spacing between ferromagnetic bonds.[15]

III. HARMONIC MAGNONS

The equilibrium spin configurations discussed in Sec. II are the starting point for the calculation of the spin excitations in the linear approximation. As shown in Ref. 12, these excitations, which we refer to as harmonic magnons, are the eigenvalues of a dynamical matrix of dimension $2N\times 2N$ obtained by linearizing the equations of motion about the equilibrium spin orientations. Because of computational considerations, the diagonalization was limited to arrays of size 24×24.

In Fig. 2 we show the distribution of magnon modes for $c=0.01$, 0.05, and 0.10 in a system where $K/J=3$. The histogram displays the combined data from three

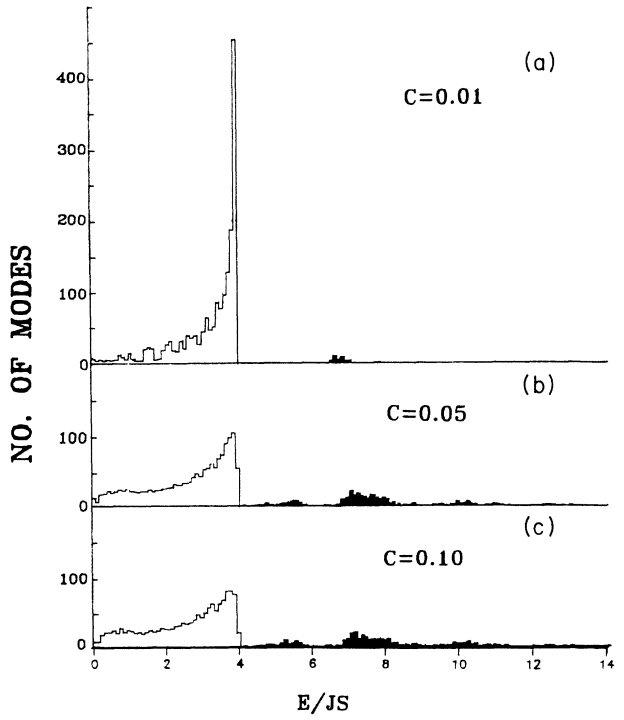

FIG. 2. Distribution of magnon modes for $K/J=3$. Data shown are from three configurations with a fraction, c, of randomly distributed ferromagnetic exchange interactions in an array of 24×24 spins. (a) $c=0.01$, (b) $c=0.05$, (c) $c=0.10$. Note change in vertical scale.

configurations of randomly distributed ferromagnetic interactions. The data for $c=0.01$ show the characteristic distribution of a two-dimensional Heisenberg antiferromagnetic, which has a peak at $E=4JS$, along with a small number of high-energy modes at $E\approx(6-7)JS$. With increasing c, the peak at $4JS$ decreases in amplitude and more modes appear at high energies.

Information about the localization of the magnon modes can be obtained from the localization indices (or inverse participation ratios) defined by[12]

$$L_\nu=\sum_{i=1}^{N}(a_{i\nu}^2+b_{i\nu}^2)^2\Big/\left[\sum_{i=1}^{N}(a_{i\nu}^2+b_{i\nu}^2)\right]^2 , \tag{6}$$

where $a_{i\nu}$ and $b_{i\nu}$ are expansion coefficients of the νth mode at the site of the ith spin. Broadly speaking, the reciprocal of L is a measure of the number of sites on which the magnon mode has significant amplitude. Thus, small values of L, $L\sim N^{-1}$, are associated with extended states, whereas values of $L\gtrsim 0.1$ characterize modes where the amplitude is confined to a relatively small number of sites (e.g., $\lesssim 10$).

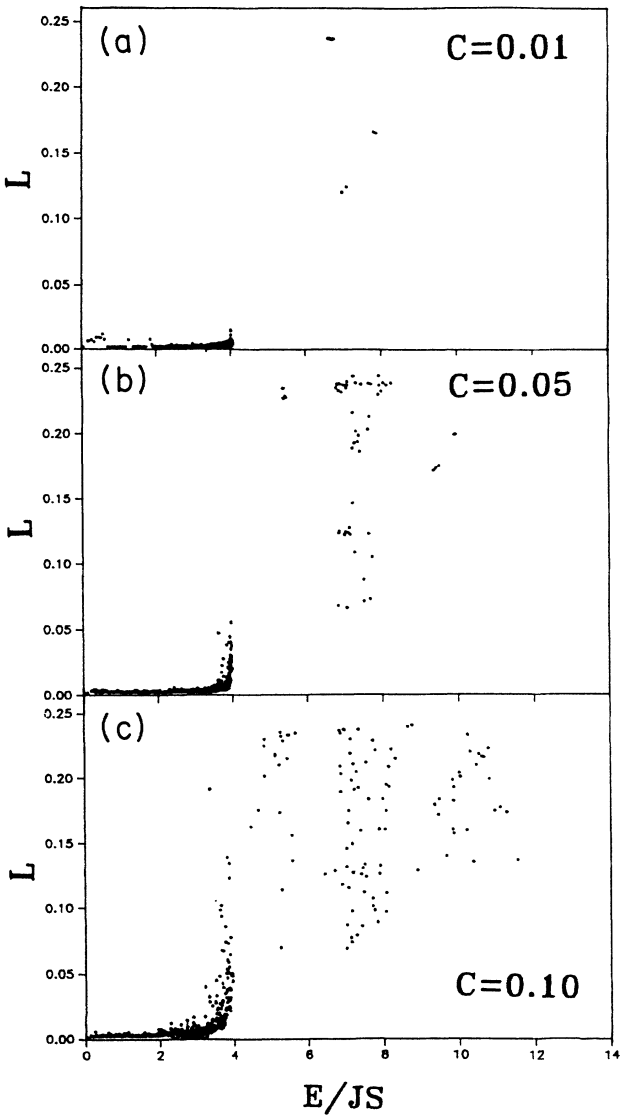

FIG. 3. Localization indices, Eq. (6), for $K/J=3$. Data shown are from one configuration with a fraction, c, of randomly distributed ferromagnetic exchange interactions in an array of 24×24 spins. (a) $c=0.01$, (b) $c=0.05$, (c) $c=0.10$.

Values of the localization indicates of single configurations of spins with $K/J=3$ and $c=0.01$, 0.05, and 0.10 are plotted in Fig. 3. Two features of the data are immediately evident. First, the high-energy modes are strongly localized, and, second, the modes at the top of the spin-wave band become more localized as c increases.

Due to the fact that the modes above $4JS$ are strongly localized, one can use a local field picture to account for their energies. In this picture, the magnon energy is equal to the Zeeman energy in the local field, i.e.,

$$E_M=\left|\sum_j J_{ij}\langle \mathbf{S}_j\rangle\right| . \tag{7}$$

When $c=0.01$, the modes in the neighborhood of $6JS$ are associated with spins which have one ferromagnetic interaction and three antiferromagnetic interactions. In the simplest approximation, the two spins connected by the ferromagnetic exchange are parallel, whereas the antiferromagnetically coupled spins are antiparallel. In such a situation

$$E_M=(3+K/J)JS , \tag{8}$$

so that $E_M=6JS$ when $K/J=3$. With increasing concentrations of ferromagnetic bands, the spins are no longer approximately colinear so that the eigenvalue distribution broadens into a band. In addition, modes appear which are associated with spins that have two or more ferromagnetic interactions.

IV. DYNAMIC STRUCTURE FACTOR

As discussed in Ref. 16, numerical calculations of the zero-temperature dynamic structure factor $S(\mathbf{q},E)$,

$$S(\mathbf{q},E)=S_{xx}(\mathbf{q},E)+S_{yy}(\mathbf{q},E)+S_{zz}(\mathbf{q},E) ,$$

can be carried out for finite arrays of spins. The calculations involve the integration of the linearized equations of motion for the boson Green's functions that are derived by carrying out a Holstein-Primakoff expansion about the equilibrium spin configurations obtained through the minimization procedure outlined in Sec. II. The results of such calculations for a 40×40 array are shown in Figs. 4 and 5 for $c=0.0$ and $c=0.01$, 0.05, and 0.10, respectively. The q values span the range from (π,π), the antiferromagnetic superlattice point, to $\frac{3}{2}(\pi,\pi)$, the boundary of the antiferromagnetic (AFM) Brillouin zone, according to the equation $\mathbf{q}=(2\pi/40)(n,n)$, with $n=21$, 22, 23, 25, 27, and 30. All curves are normalized to the same area.

In the data for $c=0$ (Fig. 4), the peaks follow the dispersion curve for the ideal square antiferromagnet where the spin-wave energy is given by

$$E(\mathbf{q})=4JS[1-\tfrac{1}{4}(\cos q_x+\cos q_y)^2]^{1/2} . \tag{9}$$

In the undoped system, the finite width of the peaks

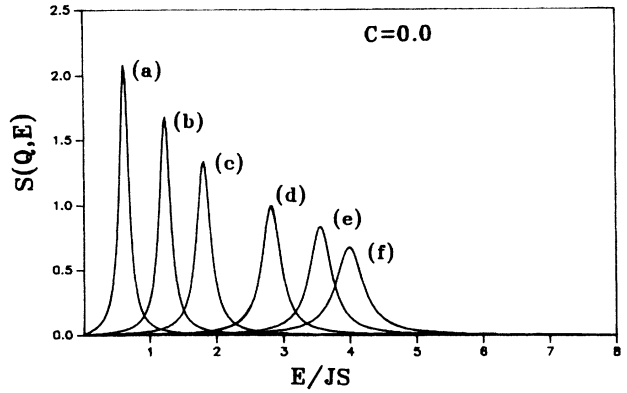

FIG. 4. Dynamic structure factor for an ideal square antiferromagnet. 40×40 array. Curves labeled (a)–(f) correspond different $\mathbf{q}$ values according to (a) $\mathbf{q}=(2\pi/40)(21,21)$, (b) $\mathbf{q}=(2\pi/40)(22,22)$, (c) $\mathbf{q}=(2\pi/40)(23,23)$, (d) $\mathbf{q}=(2\pi/40)(25,25)$, (e) $\mathbf{q}=(2\pi/40)(27,27)$, and (f) $\mathbf{q}=(2\pi/40)(30,30)$. All curves are normalized to the same area.

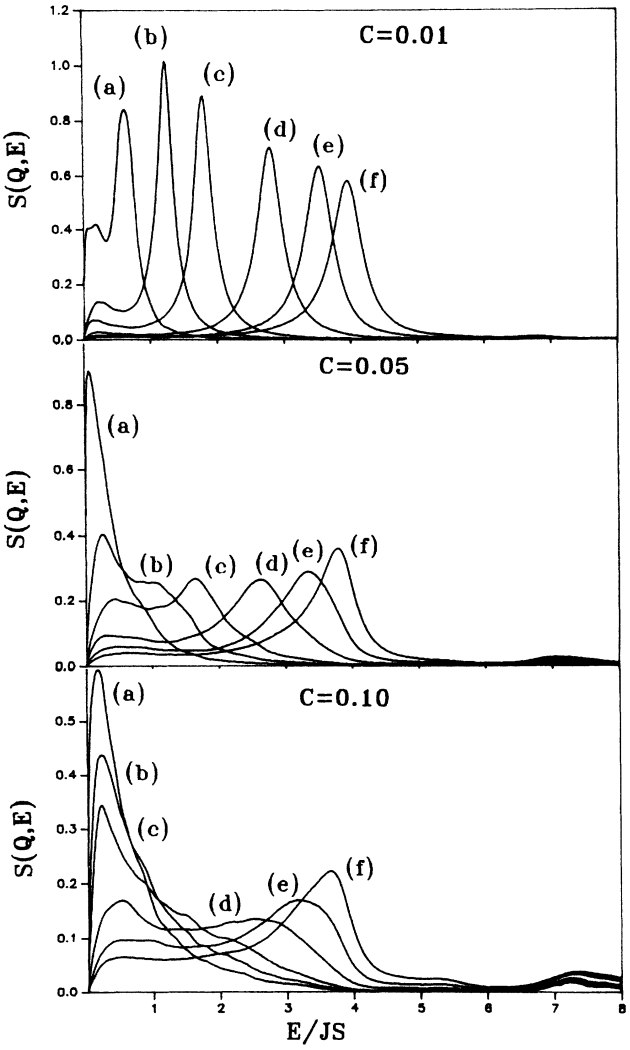

FIG. 5. Dynamic structure factor for a 40×40 array. Data shown are from a single configuration with a fraction, c, of randomly distributed ferromagnetic interactions. $K/J=3$. Labeling of the curves is the same as in Fig. 4. Cutoff parameters are as described in text.

arises from the exponential cutoff, $\exp(-\alpha t)$, in the Fourier sine transform leading to the dynamic structure factor.[16] As discussed in Ref. 16, a cutoff factor is needed to smooth out the oscillations arising from the finite interval of integration. The optimal choice of α depends on the characteristic frequency and, thus, on $\mathbf{q}$. Writing $\mathbf{q}$ as before, $(2\pi/40)(n,n)$, we used the following (n,α) pairs: (21,0.083), (22,0.010), (23,0.125), (25,0.167), (27,0.200), and (30,0.250). Note that for the pure system, the full width at half maximum of the spin-wave peak is equal to 2α.

The data for $c>0$ show that the effect of the ferromagnetic bonds is to shift and broaden the spin-wave peaks and to introduce a low-energy tail which has a tendency to rise near $E=0$. At $c=0.10$, in the case of the wave vectors near the superlattice point, curves (a)–(c), the buildup in the intensity near the origin dominates the spectrum, whereas for curves near the AFM zone boundary, curves, (d)–(f), the spin-wave peak is still prominent. [As a point of reference, the modes labeled (a)–(f) in Fig. 5 are associated with the Q points in Fig. 1 according to (a) $Q=0.05$, (b) $Q=0.10$, (c) $Q=0.15$, (d) $Q=0.25$, (e) $Q=0.35$, and (f) $Q=0.50$.] An analysis of the data shows that the modes which are most strongly damped are the ones whose wave vectors are approximately within an inverse correlation length of the superlattice point, i.e., modes for which $|\mathbf{q}-(\pi,\pi)|^2 \lesssim \kappa$.

The broadening of the spin-wave peaks in the dynamic structure factor reflects the fact that the wave-vector Q is no longer a good quantum number when the system lacks translational symmetry. The inelastically scattered neutron excites a number of magnon modes rather than the single mode excited in a translationally invariant system. For this reason, the peaks can be looked upon as being *inhomogeneously* broadened in contrast to the spin-wave peaks in systems without bond disorder, which are *homogeneously* broadened at finite temperatures due to magnon-magnon interactions.

Although many of the spectra are seen to have peaks at low energies, i.e., $E<0.5$, these are likely to be an ar-

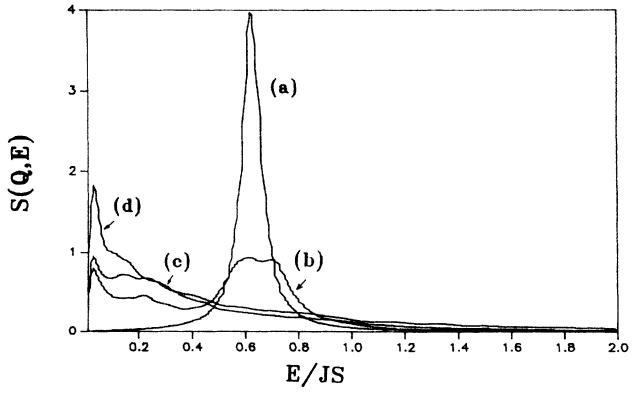

FIG. 6. Dynamic structure factor at $\mathbf{q}=(2\pi/40)(21,21)$. Data shown are from single configurations of a 40×40 array with a fraction, c, of randomly distributed ferromagnetic bands. (a) $c=0.0$, (b) $c=0.01$, (c) $c=0.05$, (d) $c=0.10$. $K/J=3$, $\alpha=0.04$. All curves are normalized to the same area. The cutoff parameter is $\alpha=0.042$.

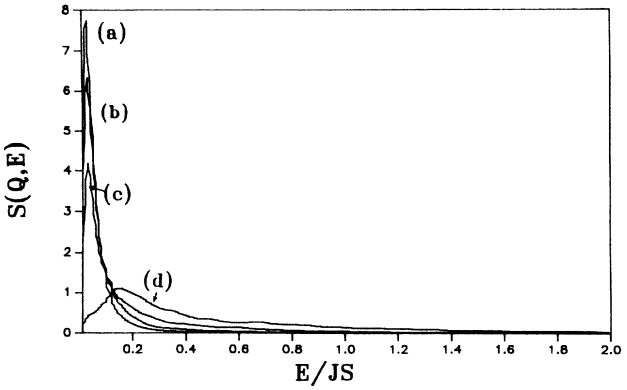

FIG. 7. Dynamic structure factor is at $\mathbf{q}=(\pi,\pi)$, the antiferromagnetic superlattice point. Parameters and labeling of the curves are the same as in Fig. 6.

tifact of the numerical calculations which force the structure factor to fall to zero at $E=0$ in an interval of width α.[16] We have explored this point in a high-resolution calculation of the structure factor in the neighborhood of the superlattice point. Figure 6 shows the results obtained with $\alpha=0.042$ at the point $(2\pi/40)(21,21)$. Curve (a) is the spin-wave peak in the undoped system and thus has an intrinsic width 2α. The spin-wave peak is still present, albeit broadened, for $c=0.01$. In addition, there is significant intensity below $0.2JS$. Curves (c) and (d) show the spectra for $c=0.05$ and 0.10, respectively. The spin-wave peak has disappeared and the intensity rises below 0.1, before falling to zero as discussed above. Figure 7 shows the data at the superlattice point, (π,π). For $c=0.0$, 0.01, and 0.05, the intensity is strongly peaked at $E=0$ (in the limit $\alpha\rightarrow 0$). In contrast, the data for $x=0.10$ suggest the possible existence of a nonpropagating AFM resonance-like mode with an energy equal to $0.15JS$.

Although there is limited inelastic neutron-scattering data available for doped La_2CuO_4, our results are qualitatively consistent with the findings of Ref. 4 for $La_{1.95}Ba_{0.05}CuO_4$ in that, relative to La_2CuO_4, the low-energy spin-wave modes are overdamped, whereas the higher-energy modes are shifted to lower energies and broadened.

V. DISCUSSION

The principal result to emerge from our calculations is that the random-bond model proposed in Ref. 1 gives a good account of the magnetic properties at low temperatures in the *insulating* phase of $La_{2-x}Sr_xCuO_4$. It reproduces the crossover from antiferromagnetic to spin-glass behavior,[1] the broadening of the static structure factor,[15] and the renormalization of the spin-wave modes seen in the related compound $La_{1.95}Ba_{0.05}CuO_4$.[4] With our choice for the ratio K/J, the changes that occur with increasing c come more slowly but on the same scale as the changes in $La_{2-x}Sr_xCuO_4$ seen with increasing Sr concentration. Although this difference may reflect the approximations inherent in the model Hamiltonian, it is also possible that the neglect of quantum fluctuations in our calculations weakens the effects of the random bands.

Our results contrast with what could have been obtained had we assumed that holes in the Cu-O planes formed singlet states with the Cu^{2+} spins. In this picture, doping with Sr introduces magnetic vacancies. In the insulating regime, the vacancies are static, and the equivalent spin Hamiltonian is that of a dilute Heisenberg antiferromagnet. Although the effect of dilution on the ground state of the two-dimensional spin-$\frac{1}{2}$ Heisenberg antiferromagnet does not seem to have been studied in any detail, it appears unlikely that there would be a crossover from antiferromagnetic to spin-glass-like behavior in the region $x \lesssim 0.06$.[17–19]

Finally, it must be emphasized that our analysis has been based entirely on the spin Hamiltonian for the Cu^{2+} lattice. The effect of adding holes to the Cu-O planes, in so far as the magnetic properties are concerned, is assumed to be accounted for by modifying the parameters of the spin Hamiltonian. It appears that such an approach is an adequate first approximation for the insulating regime where the holes are immobile at low temperatures. How the system behaves at high tempertures when thermally activated hopping is important or at high hole concentrations, when the system is metallic, is beyond the scope of the model.

ACKNOWLEDGMENTS

Research supported in part by the Weldon Springs Endowment Fund. Computer time on he Cray X-MP was provided by the Office of Basic Energy Sciences of the Department of Energy.

[1] A. Aharony, R. J. Birgeneau, A. Coniglio, M. A. Kastner, and H. E. Stanley, Phys. Rev. Lett. **60**, 1330 (1988).
[2] R. J. Birgeneau, M. A. Kastner, and A. Aharony, Z. Phys. B **71**, 57 (1988).
[3] K. Lyons *et al.*, Phys. Rev. B **37**, 2353 (1988).
[4] G. Aeppli *et al.*, Phys. Rev. Lett. **62**, 2052 (1989).
[5] V. J. Emery, Phys. Rev. Lett. **58**, 2794 (1987); see also V. J. Emery and G. F. Reiter, Phys. Rev. B **38**, 4547 (1988).
[6] F. C. Zhang and T. M. Rice, Phys. Rev. B **37**, 3759 (1988).
[7] D. L. Huber and W. Y. Ching, J. Appl. Phys. (to be published).
[8] J. D. Reger and A. P. Young, Phys. Rev. B **37**, 5978 (1988).
[9] A. Auerbach and D. P. Arovas, Phys. Rev. Lett. **61**, 617 (1988); see also T. Oguchi, Phys. Rev. **117**, 117 (1960); T. Becher and G. F. Reiter, Phys. Rev. Lett. **63**, 1004 (1989); **64**, 109 (1990).
[10] T. M. Giebultowicz *et al.*, Phys. Rev. B **39**, 6857 (1989).
[11] W. Y. Ching and D. L. Huber, Solid State Commun. **68**, 723 (1988).
[12] L. R. Walker and R. E. Walstedt, Phys. Rev. Lett. **38**, 514 (1977); Phys. Rev. B **22**, 3816 (1980).
[13] G. N. Parker and W. M. Saslow, Phys. Rev. B **38**, 11 718 (1988); W. M. Saslow and G. N. Parker, *ibid.* **38**, 11 722 (1988); J. Appl. Phys. (to be published).

[14]J. Vannimenus, S. Kirkpatrick, F. D. M. Haldane, and C. Jayaprakash, Phys. Rev. B **39**, 4634 (1989).
[15]R. J. Birgeneau *et al.*, Phys. Rev. B **38**, 6614 (1988).
[16]W. Y. Ching, D. L. Huber, and K. M. Leung, Phys. Rev. B **23**, 6126 (1981).
[17]H. Kitazawa, K. Katsumata, E. Torikai, and K. Nagamine, Solid State Commun. **67**, 1191 (1988).
[18]D. R. Harshman *et al.*, Phys. Rev. B **38**, 852 (1988).
[19]J. I. Budnick *et al.*, Phys. Rev. Lett. **62**, 102 (1989).